

In-vivo IVUS Tissue Classification A Comparison Between Normalized Image Reconstruction and RF Signals Analysis

Karla L. Caballero¹, Joel Barajas¹, Oriol Pujol^{1,2}, Josefina Mauri³, Petia Radeva¹

1 Computer Vision Center, Universitat Autònoma de Barcelona, Bellaterra, Spain

2 Dept. Matemàtica Aplicada i Anàlisi, University of Barcelona, Barcelona, Spain

3 Hospital Universitari German Trias i Pujol, Badalona, Spain

E-mail: kcaballero@cvc.uab.es

Abstract In this paper we present a novel framework for classification of the different kind of tissues in intravascular ultrasound (IVUS) data. We describe a normalized reconstruction process for IVUS images from radio frequency (RF) signals. The reconstructed data is described in terms of texture based features and feeds an ECOC-Adaboost learning process. In the same manner, the RF signals are characterized using Autoregressive models, and classified with a similar learning process. A comparison is performed among these techniques using two different cross validation schemes: 50 rounds of 90-10-Holdout and Leave One Patient Out obtaining very promising results.

1 Introduction

Plaque rupture is one of the most frequent causes of acute coronary syndromes. Nowadays, there are many studies which report a high correlation between multiple plaque ruptures and myocardial infarction. Intravascular ultrasound (IVUS) offers the opportunity to study the morphology and the histological properties of the arterial plaque from a vessel cross-section view. The automatic analysis of the IVUS images is significant to elaborate a proper diagnosis, since it is a suitable technique to predict and quantify vulnerable plaques and different tissues on the vessel walls, preventing the subjectivity of the physician who performs the study.

The analysis of IVUS data has been approached in two ways: on one hand, the examination of the DICOM images is performed by a texture analysis [15, 14]. The main drawback of this approach is the great variability in appearance among the tissues of different patients due to diverse parameterizations

in the reconstruction process. On the other hand, in order to avoid this problem the original radio-frequency (RF) signal is exploited [7, 6, 10]. This last approach is difficult to characterize and lacks robust description tools when compared to the image based analysis. Nevertheless, the dominance of one technique over the other has not been reliably assessed using the same data set.

The contributions of this paper are three-fold: firstly, we propose a method that takes advantage of both tendencies to solve the problem of parameterizations diversity. This method is based on the reconstruction of normalized IVUS images from the radio frequency signal, and the application of image based characterization processes. Secondly, we suggest a framework based on Error Correcting Output Codes (ECOC) combined with Adaboost [3] as a base classifier to categorize both, RF signals and texture-based descriptors. Finally, we perform a statistical comparison between both techniques using two cross validation schemes. In order to compare the accuracy of the different tissue classification approaches, we use 100 rounds of holdout, which is one of the most widely used techniques in literature. On the other hand, Leave One Patient Out allows us to highlight the prediction behavior of each technique by reducing the bias in the classification rates in front of unseen patients.

The layout of the article is as follows: in section 2, we present the normalized image reconstruction process. In section 3, RF signal analysis and characterization is explained. Section 4 exposes the process of texture features extraction. The classification and validation schemes used are described in section 5. Finally, the results, discussion, and conclusion are presented.

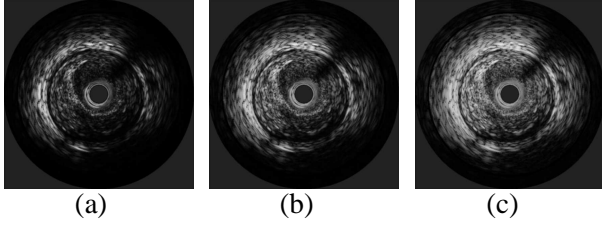


Figure 1: Reconstructed IVUS images from RF signals with different DDP gain parameters. (a)DDP gain parameter fixed to 1.04. (b)DDP gain parameter fixed to 2.20. (c)DDP gain parameter fixed to 3.00.

2 Image Reconstruction Process

The IVUS catheter carries an ultrasound emitter which shoots a given number of beams, and a transducer that collects their reflections as RF signals. Based on the kind of tissue, these echoes vary their frequency and amplitude. The RF signals are acquired using a 12-bit acquisition card with a sampling rate of $200MHz$. The IVUS equipment used was a Galaxy II from Boston Scientific with a catheter transducer frequency of $40MHz$. It is assumed a sound propagation in tissue of $1565m/s$. Each IVUS image consists of a total of 256 A-lines (ultrasound beams) [8], with a length of $6.5mm$. Each RF data is acquired from an *in vivo* patient pull-back sequences.

Once the RF data has been acquired, an image construction framework is applied to obtain IVUS images with a same parameter set. Firstly, the signals are filtered, and linear time gain compensation is applied in order to correct the tissue attenuation $\alpha = 1Db - MHz/s$. Then, a signal envelope is calculated using the Hilbert transform. This envelope is compressed in a logarithmical form to distribute the image gray levels and to enhance the image visualization, then is normalized from 0 to 1. The image is transformed to cartesian coordinates, and the missing pixels between each angle are obtained using a bilinear interpolation. Finally, a non linear Digital Development Process (DDP) to regulate the contrast radially is applied [4]. With these parameters we can normalize all the images to obtain the same contrast with low computational cost, which is not an easy duty in DICOM images since the parameter set is not saved. Figure 1 shows an example of constructed images with different gain parameter values.

3 RF Signal Analysis by means of AR models

Once the RF signals have been acquired, filtered at the transducer frequency, and linearly compensated in the time, a characterization process is performed. According to [9, 6], one of the most suitable methods to analyze ultrasound signals is to model their power spectrum using Autoregressive (AR) models.

The autoregressive models are defined as a linear prediction equation where the output x at a certain point n is equal to a linear combination of its previous outputs p with a given weight a_p [13].

$$x(n) = \sum_{k=1}^p a_p(k)x(n-k),$$

The AR models are used to approximate the power spectrum of a RF signal window. First, a Power Spectrum is modelled using A-line section of n samples, then an average for a given window is obtained allowing a single 1-D AR model for the entire section as it is shown in figure 2. In our case, it is composed of 64 samples and 12 of the 256 A-lines. Note that only one side of the spectrum is used because of its symmetry. The power spectrum data set is composed of 200 sampled frequencies ranging from 0 to $100MHz$, each value of the spectrum is used as a feature for classification. Additionally, an sliding window of 64 samples and 12 A-lines, and a displacement of 16 samples and 4 A-lines are used to increase the resolution of characterization.

4 Texture Features Extraction

We have extracted image features with 3 different texture descriptors: Co-occurrence Matrix, Local Binary Patterns and Gabor Filters.

4.1 Co-occurrence Matrix

The co-occurrence matrix is defined as the estimation of the joint probability density function of gray level pairs in an image [12]. The sum of all element values is:

$$P(i, j, D, \theta) = P(I(l, m) = i \otimes I(l + D\cos(\theta), m + D\sin(\theta)) = j),$$

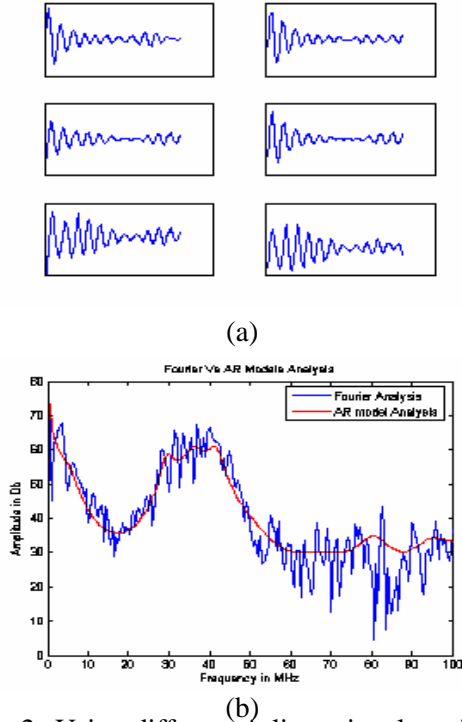


Figure 2: Using different A-lines signal sections (a) to create an unique Autoregressive model(b)

where $I(l, m)$ is the gray value at pixel (l, m) , D is the distance among pixels and θ is the angle between neighbors. The most common values for the orientation θ are $[0^\circ, 45^\circ, 90^\circ, 135^\circ]$, [5, 12]. After computing this matrix, some descriptive measures such as Energy, Entropy, the Inverse Difference Moment, Shade, Inertia and Promenace are extracted [12]. Thus, a 48 feature space is built for each pixel, since we are estimating 6 different measures at 4 orientations and two distances $D = [5, 8]$.

4.2 Local Binary Patterns

Local Binary Patterns are used to detect uniform texture patterns in circular neighborhoods with any quantization of angular space and spatial resolution[11]. It is based on a circular symmetric neighborhood of P members with radius R . To achieve gray level invariance, the central pixel g_c is subtracted to each neighbor g_p , assigning the value 1 to the result if the difference is positive and 0 otherwise. Hence, LBP is defined as follows,

$$LBP_{R,P} = \sum_{p=0}^{P-1} s(g_p - g_c) \cdot 2^p$$

These operators generate a 3 dimensional space by applying a radius of $R = [1, 2, 3]$ and a neighborhood

of $P = [8, 16, 24]$.

4.3 Gabor Filters Bank in Texture analysis

The Gabor Filters is an special case of wavelets [2], and is essentially a Gaussian g modulated by a complex sinusoid s . In 2D, a Gabor filter has the following form in the spatial domain:

$$h(x, y) = \frac{1}{2\pi\sigma^2} \exp\left\{-\frac{1}{2}\left[\frac{x^2+y^2}{\sigma^2}\right]\right\} \cdot s(x, y),$$

$$s(x, y) = \exp[-i2\pi(Ux + Vy)] \quad \phi = \arctan V/U$$

where σ is the standard deviation, U and V represent the 2D frequency of the complex sinusoid, and ϕ is the angle of frequency. We use a polar representation, F, ϕ , of the 2D cartesian frequency, (U, V) . Thus, we have created a filter bank using the following parameters:

$$\sigma = [12.7205, 6.3602, 3.1801, 1.5901],$$

$$\phi = [0^\circ, 45^\circ, 90^\circ, 135^\circ],$$

$$F = [0.0442, 0.0884, 0.1768, 0.3536],$$

As a result a feature vector of 67 dimensions for each pixel is obtained, which will be used to train the classifier.

5 Classification

Once we have designed a characterization framework for reconstructed images and RF signals, a classification scheme is developed. We establish 3 classes of tissues: fibrotic plaque, lipid or soft plaque, and calcium. We have used the Adaptive Boosting (Adaboost) [16, 3] as the supervised learning technique.

Since we have a multiclass problem, we need to establish some combination criterium for the classifier output. To solve it we have employed the Error Correcting Output Codes technique (ECOC)[1].

ECOC consists in assigning a code map table which relates the classifiers outputs with the classes. Then, the final classification is obtained by finding the minimum Euclidean distance between the resulting code and the classes code. The classification map from the ECOC is the same for both techniques, which it is shown in table 1. Here, the 0 values indicate that these classes are not used in the selected classifier. The 1's indicate that the classifier should output a positive value when this class is found, and negative one (-1) when it is not.

Table 1: ECOC code map used in the classification

Classes	Classifier	Classifier	Classifier
—	1	2	3
Calcium	1	1	0
Fibrotic Plaque	-1	0	1
Soft Plaque	0	-1	-1

We have used to schemes to perform the classification validation: 50 rounds of 90-10-holdout and leave one patient out cross-validations. We test for statistical significance by applying a two-tailed t-test with a confidence level of 95%. The first scheme, the holdout cross-validation, helps us to assess the mean error and confidence intervals of the classification process. However, it does not measure the prediction capacity of the learning method in front of unseen patients. In order to solve this problem, the leave one patient out scheme is used. This method trains the learning technique with all but one patient, leaving this last one for testing purposes.

6 Results

We have obtained the RF signals and their reconstructed images *in vivo* from a set of 10 patients pullbacks acquired in the German Trias i Pujol Hospital from Badalona Spain. All of these pullbacks contain the three classes of plaque. For each one, 10 to 15 different vessel sections are selected to be analyzed.

The physicians have segmented from the vessel images around of 50 areas of interests per patient. From these segmentations we have taken 500 regions of interest (ROI) per patient and tissue randomly making a total of 15000 evaluation ROIs. To build the data set, these selections were mapped in both RF signals and reconstructed images.

6.1 Gain Assessment

In order to test the performance of our texture based classification approach, we have selected 6 different DDP gain parameters to reconstruct the images. Thus, six different data sets have been created and their extracted texture features have been processed separately. For every DDP gain parameter values a classification error has been computed for each kind of tissue. The accuracy for different DDP gain para-

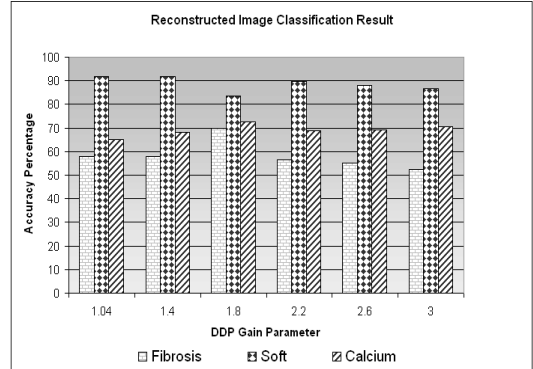


Figure 3: Classification result among different DDP gain parameters for each type of tissue with Leave One Patient Out Method

Table 2: Classification Results from RF Signal Analysis and Texture Based Analysis with Holdout and Leave One Patient Out (LOPO) methods

Classes	RF Signal Analysis	
	Holdout	LOPO
Fibrosis	84.22% ± 0.44	76.41% ± 8.50
Soft	86.22% ± 0.41	81.2% ± 6.89
Calcium	88.60% ± 0.49	83.35% ± 5.38

Classes	Texture Base Analysis	
	Holdout	LOPO
Fibrosis	76.38% ± 0.68	70% ± 9.67
Soft	87.29% ± 0.44	83.5% ± 6.46
Calcium	76.04% ± 0.74	72.6% ± 12.94

meters with the Leave One Patient Out is shown in figure 3.

It can be seen that the best gain parameter is 1.8 where the classification results are: 70% for fibrotic plaque, 83.2% for lipid, and 72.6% for calcium with the Leave One Patient Out.

6.2 Classification Comparison

We have tested both RF and normalized image reconstruction based characterization with the two cross-validation schemes presented. Table 2 shows a comparative of their performance. Notice that these results have been obtained with pixel resolution in both schemes, without any kind of postprocessing.

It can be observed that the RF signal modelling

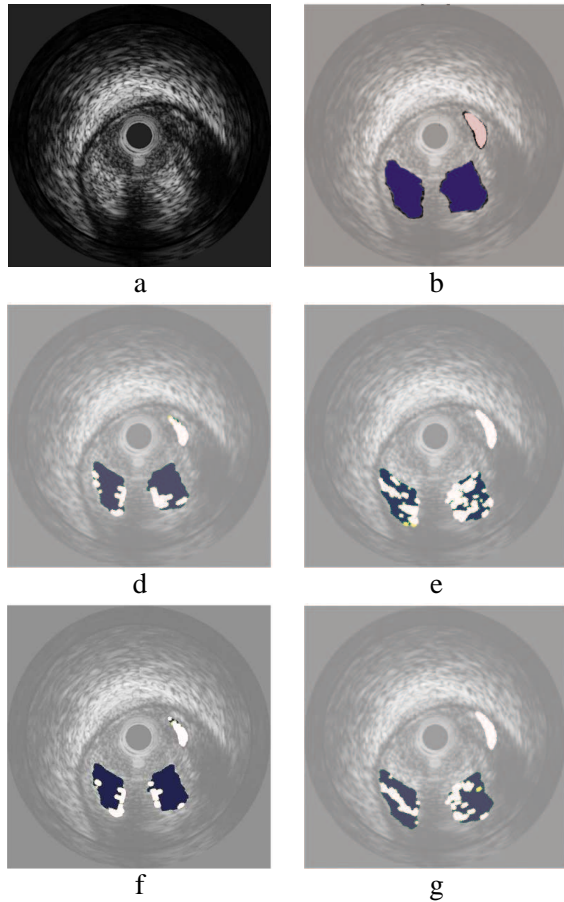


Figure 4: Images (a) IVUS cross sectional (b) Segmented by the physician. (c) Classified with RF signal Analysis with Leave One Patient Out method. (d) Classified with Texture Based Features and Leave One Patient Out. (e) Classified with RF Signal Analysis and Holdout method. (f) Classified with Texture Based and Holdout. Dark regions represent fibrous plaque, and white regions means lipid plaque and light gray is calcium.

attains a higher accuracy in both validation tests. Moreover, the inter-patient variability is lower than in the case of image-based analysis and has a better prediction behavior in front of unseen patients. However, the accuracy rates obtained by the normalized reconstruction process represents a significant improvement when compared to the DICOM based tissue characterization - in this kind of images the accuracy is around 76% without any kind of post-processing [14]. This result lead us to believe that the gain normalization process is a necessary step in image based tissue characterization.

Figure 4 shows some results in an unseen patient.

Figures 4(c)(e) depict the results using a holdout training model and a leave one patient out training model for the RF signal. Observe that the differences between them are not significant. Additionally, figure 4(d)(f) shows the same results for the image based texture characterization model. Note that the qualitative accuracy of this last technique is lower than in the RF case.

7 Discussion and Conclusion

Two methods for tissue classification in IVUS from *in vivo* patients have been presented taking into account three types of plaque: fibrotic, soft, and calcium. We have proposed a more accurate technique for image tissue assessment based on a set of normalized data, which is not possible in conventional approaches based on DICOM images. To do so, an image reconstruction method has been depicted.

We have compared the RF signal with the image-based tissue characterization. The results show that RF signal is more suitable for this task in terms of mean error rate as well as prediction accuracy. These results have been obtained using two cross-validation schemes: repeated holdout and leave one patient out. The classification presented here has been done for each pixel without any kind of postprocessing, since we desire to preserve the highest possible resolution. Some grouping techniques and the inclusion of other features could be applied to the obtained results in order to improve the classification.

Despite this results, we consider that the image based tissue characterization is not to be overlooked. In fact we believe that a combination of multiple DDP gain values, one for each tissue, could be suitable to enhance the performance.

As a future line we are planning to combine both characterization frameworks in order to take advantage of the high accuracy from the RF signal and the high amount of description techniques available in image based analysis.

Acknowledgements

This work is supported in part from projects FIS-G03/1085, FIS-PI031488, TIC2003-00654 and MI-1509/2005, the Generalitat de Catalunya under the

FI grant REF 2006FI 00216 and the MEC under the FPU grant AP2005-0926.

References

- [1] E. L. Allwein, R. E. Schapire, and Y. Singer. Reducing multiclass to binary: A unifying approach for margin classifiers. *Journal of Machine Learning Research*, 1.
- [2] J.G. Daugman. Uncertainty Relation for Resolution in Space, Spatial Frequency, and Orientation Optimized by Two-Dimensional Visual Cortical Filters. *Journal of the Optical Society of America*, 2(A):1160–1169, 1985.
- [3] J. Friedman, T. Hastie, and R. Tibshirani. Additive logistic regression: a statistical view of boosting. *Annals of Statistics*, 28:337–374, 2000.
- [4] R. Gonzales and R. Woods. *Image Processing*. Adison - Wesley, 1992.
- [5] T. Randen J. H. Husoy. Filtering for texture classification: A comparative study. *IEEE Transactions on Pattern Analysis and Machine Intelligence*, 4:291–310, 1999.
- [6] T. Iwamoto, A. Tanaka, Y. Saijo, and M. Yoshizawa. Coronary plaque classification through intravascular ultrasound radiofrequency data analysis using self-organizing map. In *IEEE Ultrasonics Symposium*, pages 2054–2057, 2005.
- [7] A. Jeremias, M. Kolz, T. Ikonen, J. Gummert, and A. Oshima. Feasibility of in vivo intravascular ultrasound tissue characterization in the detection of early vascular transplant rejection. *Circulation*, 100:2127–2130, 1999.
- [8] G.S. Mintz, S. E. Nissen, and W. D. Anderson. American college of cardiology clinical expert consensus document on standards for acquisition, measurement and reporting of intravascular ultrasound studies (ivus). *Journal of the American College of Cardiology*, 37:1478–1492, 2001.
- [9] A. Nair, B. Kuban, E. Murat, P. Schoenhagen, S. Nissen, and D. Vince. Coronary plaque classification with intravascular ultrasound radiofrequency data analysis. *Circulation*, 106:2200–2206, 2002.
- [10] A. Nair, B. D. Kuban, N. Obuchowski, and G. Vince. Assessing spectral algorithms to predict atherosclerotic plaque composition with normalized and raw intravascular ultrasound data. *Ultrasound in Medicine & Biology*, 27:1319–1331, 2001.
- [11] T. Ojala and M. Pietikainen T. Maenpaa. Multiresolution gray-scale and rotation invariant texture classification with local binary patterns. *IEEE Transactions on Pattern Analysis and Machine Intelligence*, 24:971–987, 2002.
- [12] R. Dubes P. Ohanian. Performance evaluation for four classes of textural features. *Pattern Recognition*, 25:819–833, 1992.
- [13] J. Proakis, C. Rader, F. Ling, and C. Nikias. *Advanced Digital Signal Processing*. Mc Millan, 1992.
- [14] O. Pujol. *A semi-supervised Statistical Framework and Generative Snakes for IVUS Analysis*. Graficas Rey, 2004.
- [15] O. Pujol, M. Rosales, and P. Radeva. Intravascular ultrasound images vessel characterization using adaboost. In *Functional Imaging and Modelling of the Heart: Lecture Notes in Computer Science*, pages 242–251, 2003.
- [16] R. Schapire. The boosting approach to machine learning: An overview, 2001.